Available online at www.sciencedirect.com
ScienceDirect
Journal of Power Sources 163 (2006) 392–397
JOURNAL OF POWER SOURCES
www.elsevier.com/locate/jpowsour

Short communication

Nano-composite materials for high-performance and durability of solid oxide fuel cells

Sun-Dong Kim [a], Hwan Moon [a], Sang-Hoon Hyun [a,*], Jooho Moon [a], Joosun Kim [b], Hae-Weon Lee [b]

[a] *School of Advanced Materials Science and Engineering, Yonsei University, Seoul 120-749, Republic of Korea*
[b] *Nano Materials Research Center, Korea Institute of Science and Technology, Seoul 136-791, Republic of Korea*

Received 14 June 2006; received in revised form 2 August 2006; accepted 15 September 2006
Available online 31 October 2006

Abstract

A functional composite powder containing nano-sized NiO and YSZ (8 mol% Y_2O_3–ZrO_2) co-conjugated on YSZ powder is synthesized by a Pechini-type polymerizable complex method in an effort to yield improved performance and durability in solid oxide fuel cells (SOFCs). A SOFC single cell made from the dual composite powder exhibited high power density of 1.2 W cm^{-2} and showed excellent durability (zero degradation) under a load of 1.0 A cm^{-2} during 550 h of operation at 800 °C. The durability is attributed to the uniform and constrained cermet structure, and particularly from the interface between Ni and YSZ, which has been modified via nano-conjugation. The proposed composite powder is an attractive candidate material for making homogeneous, durable, and highly efficient electrode microstructures.

Keywords: Solid oxide fuel cell; Ni–YSZ anode; Nano-composite powder; Conjugation; Durability

1. Introduction

SOFCs have been recognized for their unsurpassed efficiency and essentially pollution-free operation. In order to enter mainstream power markets, however, high reliability and economic feasibility are crucial. Recently, it has become required that SOFCs maintain life times of more than 40,000 h [1]. One important element that influences the durability of SOFCs is the microstructure stability of the electrodes during the operation [1–5]. This is particularly true for a Ni–YSZ cermet anode. Theoretical studies indicate that degradation in SOFC anodes arises from Ni rearrangement through surface diffusion, which is disadvantageous with respect to pore stabilities and three phase boundaries (TPBs) expansion [6–8]. For these reasons, researchers have attempted to develop better anodes by optimizing the cermet structure [6–18].

The main approach to optimizing the cermet structure is through preparation of electrodes by means of controlling the grain sizes of Ni and YSZ. Briefly, results have shown that the ionic resistance and TPBs of the electrode depend on the size and distribution of the constituent particles. Many experiments have been carried out using an approach that optimizes the cermet structure, although controversy exists over the optimal combination of particle sizes [6,9]. This discord arises from fundamental problems related to the homogeneity of the mix and from the process variables. Thus, obtaining the desired microstructure from a mixture containing various materials (e.g., NiO, YSZ, pore-former, organic additives) is not straightforward. Another issue lies in the nature of the thermodynamic properties between metal and ceramic. As the surface energy of nickel and YSZ exhibit fairly different values, the hetero-grains at the interface lose chemical affinity, and thus factors such as their de-wetting properties are adversely affected. Therefore, coarsening of the nickel phase proceeds appreciably due to poor adhesion of the metal to the ceramic material at elevated temperatures. It should be noted, however, that the YSZ in the cermet prevents mobility of the Ni phases [19,20].

Synthesis of dual composite powders presents a challenge that has not been met thus far. Cermet anodes comprised of dual composite powders offer the following advantages: (1) mixing homogeneity—the dual composite powder behaves as if it contains only single particles; (2) the self-creation of a porous

* Corresponding author. Tel.: +82 2 2123 2850; fax: +82 2 365 5882.
E-mail address: prohsh@yonsei.ac.kr (S.-H. Hyun).

0378-7753/$ – see front matter © 2006 Elsevier B.V. All rights reserved.
doi:10.1016/j.jpowsour.2006.09.015

structure without a pore-former—each conjugated NiO and YSZ porous layer interferes with the other's sintering process, making the porosity of the Ni–YSZ anode greater than 40% without use of a pore-former; (3) microstructural stability—aging of the electrode is controlled by a fine YSZ skeleton and the coherence between co-conjugated Ni and YSZ; (4) TPB expansion by nano-conjugation; and (5) high electrical conductivity and mechanical strength. In order to carry out meaningful investigations of a dual composite powder, the ideal powder should be made up of nano-sized NiO and YSZ co-conjugated on YSZ particles, and the performance and durability of a single cell must be assessed.

2. Experimental

2.1. Synthesis of dual composite powder

The synthetic procedure for the proposed dual composite powder follows a Pechini-type polymerizable complex method, as depicted in Fig. 1. Metal nitrates of Ni, Zr, and Y were obtained from Aldrich. An aqueous solution of $ZrO(NO_3)_2{\cdot}xH_2O$, $Y(NO_3)_2{\cdot}6H_2O$, and $Ni(NO_3)_2{\cdot}6H_2O$ was mixed by stirring with citric acid (Junsei), and heated at 60 °C for 2 h. YSZ (TZ-8YS, Tosoh) and ethylene glycol (Junsei) were then added to the aqueous solution. The polymeric solution condensed at 180 °C for 4 h and ash-colored intermediates were obtained. The resulting intermediates were calcined at 600 °C and milled in methanol to yield the dual composite powder.

2.2. Preparation of a single cell

The dual composite powder was compacted under uni-axial pressure to form a disc. The dimensions of green anode discs were 38 mm in diameter and 1.2 mm in thickness. The green anodes were pre-sintered at 1300 °C for 3 h. YSZ (TZ-8YS, Tosoh) slurry was then applied onto the anode via dip-coating and sintered at 1400 °C for 3 h to achieve a thin (<7 μm) and dense YSZ electrolyte film. The method employed for the synthesis of a thin and dense YSZ electrolyte film via dip-coating has been reported in a previous work by the authors [21]. The cathode was fabricated by screen-printing with paste materials comprised of a mixture of the powders and additives dispersed in an organic solvent mixed by a three-roll mill (EXAKT 35). $La_{0.8}Sr_{0.2}MnO_3$ (Praxair, USA) and YSZ (TZ-8YS, Tosoh) were used as cathode materials with a weight ratio of 50:50. The binder and solvent for the paste was ethyl-cellulose and α-terpineol, respectively. The cathode paste was successively applied on the anode supported electrolyte with an active area of 1.5 cm^2 and a thickness of 30 μm. The cathode layer was sintered at 1150 °C for 3 h. The current collectors for the cathode and anode side were Pt mesh and Ni felt, respectively. A small amount of platinum paste was applied between the cathode and Pt mesh in order to establish good contact.

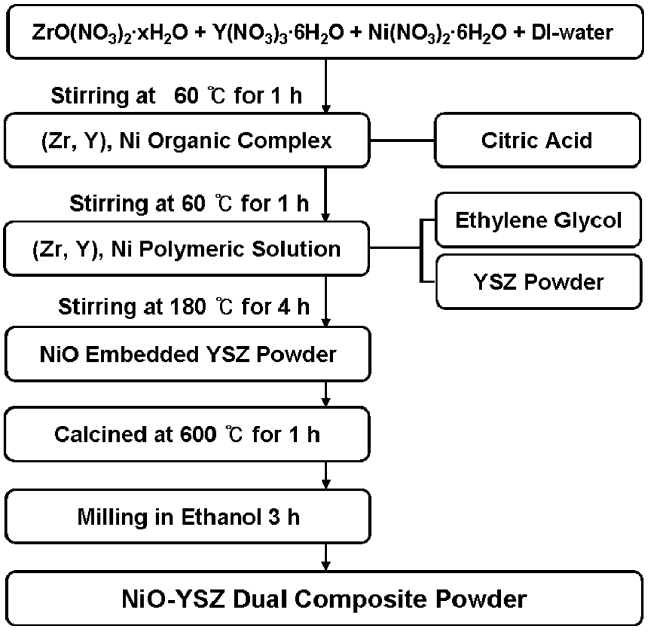

Fig. 1. Experimental flow chart for the synthesis of NiO–YSZ dual composite powder.

2.3. Characterizations and single cell tests

The crystalline phases of the materials were analyzed by X-ray diffractometry (Rint 2700, Rigaku Co., Japan). The microstructures were observed by scanning electronic microscopy (SEM; Model S4200, Hitachi, Ltd., Japan) and via an optical microscope (DLML, Leica, Germany). Transmission electron microscopy (TEM) and energy-disperse X-ray spectroscopy (EDX) were performed in order to observe the conjugated nano-phases.

The performance of the anode supported single cell was evaluated at various temperatures (600–800 °C) in reactive gases of humidified hydrogen (200 $cm^3\,min^{-1}$) with 3% H_2O at the anode side and air (300 $cm^3\,min^{-1}$) at the cathode side. The *I–V* characterization and durability were measured with a multi-functional electronic load module (3315D, Taiwan). AC impedance measurements were conducted with a Solatron 1260 frequency analyzer and a Solatron 1287 interface. The AC impedance spectra in a frequency range of 0.1–10^5 Hz with an excitation voltage of 10 mV were taken in order to ensure a linear response.

3. Results and discussion

3.1. Characteristics of dual composite powder

A dual composite powder was synthesized by polymerization and condensation of nickel, zirconium, and yttrium salts onto YSZ surfaces, applying a Pechini-type polymerizable complex method. The characteristics of yttrium and zirconium, including the atomic diameter, crystal structure, electronegativity, and valences, are extremely favorable in terms of allowing extensive solid solubility. In other words, during the synthetic procedure, there is scarce formation of an intermediate between NiO and YSZ arising from differences in atomic conditions. Shown in Fig. 2a and b is a schematic diagram and a typical scanning

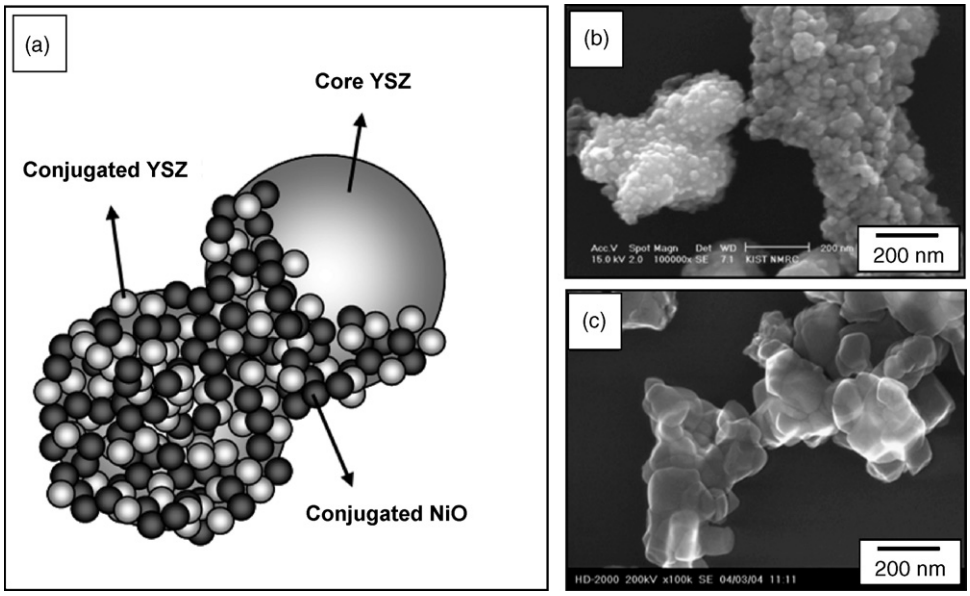

Fig. 2. (a) Schematic diagram of the dual composite powder, (b) SEM image of the dual composite powder which is composed of nano-sized NiO and YSZ co-conjugated on YSZ particle, and (c) SEM image of the commercial YSZ (TZ-8S, Tosoh) which is the core material of the dual composite powder.

electron microscopy (SEM) image of the dual composite powder, respectively. The configuration of the powder is porous and is primarily nano-sized (10–30 nm) NiO and YSZ co-conjugated on YSZ (Fig. 2c) particles. In comparison with the YSZ powder (mean diameter 0.3 μm, surface area 6.2 $m^2\,g^{-1}$) used for the core particles, the particle size and surface area of the dual composite powder is increased by 0.42 μm and 23.55 $m^2\,g^{-1}$, respectively.

The X-ray diffraction (XRD) pattern of the as-prepared dual composite powder is shown in Fig. 3a. Crystalline phases of the synthesized powder correspond precisely with those of NiO and YSZ, and show typical nano-particles shape. Through the process of sintering at 1400 °C and reduction at 800 °C in a hydrogen atmosphere, the crystallinity increased and sharp peaks for Ni and YSZ were observed without any impurities or intermediates (Fig. 3b).

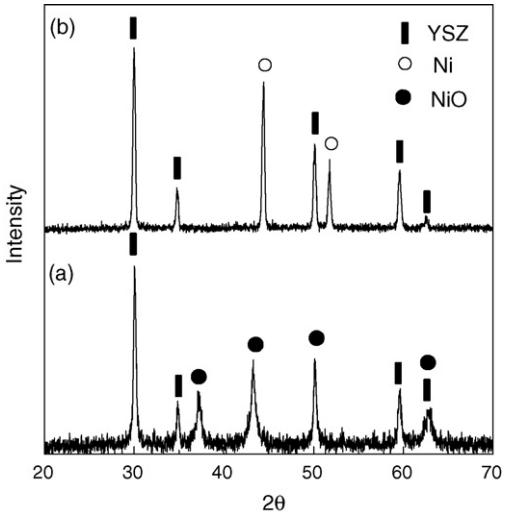

Fig. 3. X-ray diffraction patterns of (a) the as-prepared dual composite powder and (b) the EDC after sintering at 1400 °C and reduction at 800 °C of hydrogen environment.

3.2. Characteristics of electrode made of dual composite powder

All microstructure was analyzed after testing. Typical microstructure of an anode-supported single cell using an electrode made of the dual composite powder (henceforth referred to as EDC) is depicted in Fig. 4a. The cell is composed of a 30 μm LSM-YSZ cathode, a 7 μm YSZ electrolyte layer, and a 900 μm Ni–YSZ anode. The electrolyte layer is fully dense and has only a few isolated pores. Each electrode layer is very uniform without any defects. Theoretical studies show that the TPB length in an electrode is inversely proportional to the grain size and can be optimized by the pore-size and porosity [22]. Note that the grain size of the dual composite powder (<0.42 μm) is much smaller than that of commercial anode materials (few micron scale) while having a similar level of porosity and/or pore-size of electrodes. Therefore, it can be inferred that there is a considerable amount of Ni–YSZ-pore three phase boundaries (TPBs) at the contiguous region between the YSZ electrolyte and the Ni–YSZ anode.

Shown in Fig. 5 is the porosity and linear shrinkage variations of EDCs in relation to the sintering temperatures. To date, it is widely believed that a porous Ni–YSZ anode can be obtained only through the use of pore-formers, e.g., carbon, graphite, starch, etc. However, the EDC exhibits considerable porosity (>41%) without use of a pore-former, contrary to a normal sintering process [23]. This is responsible for the formation of intricate junctions between the YSZ skeleton and co-conjugated nickel oxide and YSZ phases. The presence of a heterogeneous region (i.e., an area characterized by a difference in melting point, surface energy, and mutual arrangement) in the compact reduces net shrinkage and density of the compact [24,25]. The sintering pro-

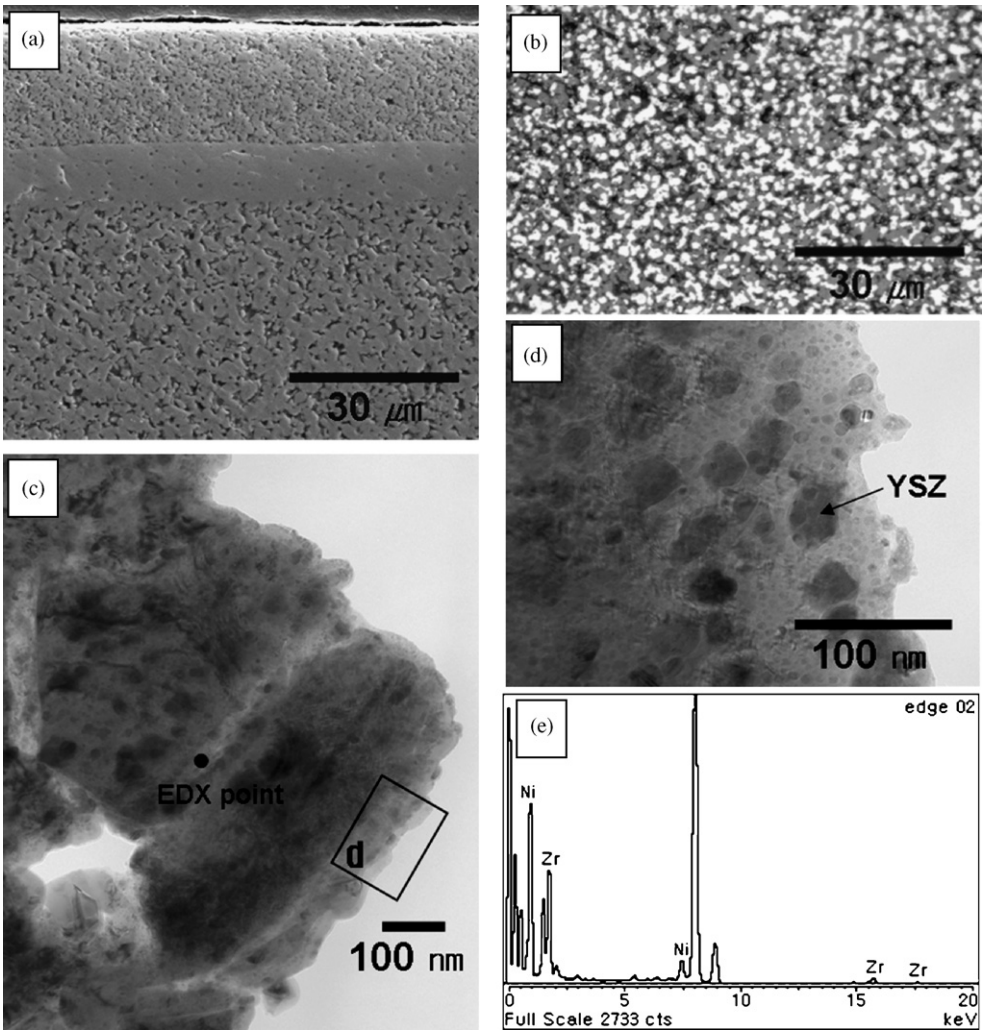

Fig. 4. (a) A cross-sectional view (SEM image) of a single cell with LSM-YSZ/YSZ/EDC, (b) optical image of EDC (white: Ni, dark gray: YSZ, and black: pore), (c) TEM image (×50 K) of the EDC (d) TEM image (×100 K) of EDC, and (e) EDX signal of EDC (at EDX point in c).

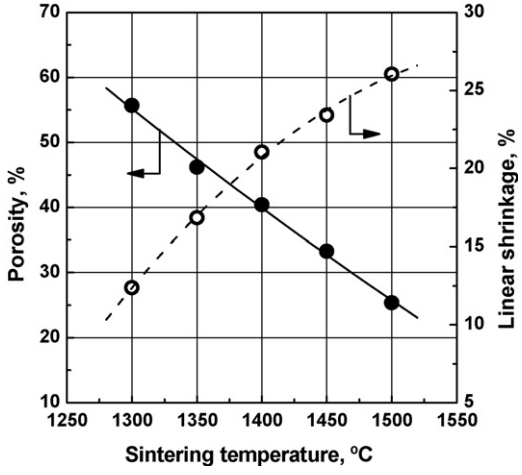

Fig. 5. Porosity and linear shrinkage variations of the EDC depending on the sintering temperatures.

cedure terminated at an intermediate stage, which results in the preservation of a desirable pore structure. The pore distribution of the EDC is uniform, and Ni (white) and YSZ (gray) phases were also homogeneous and well-connected, as can be seen in Fig. 4b. Transmission electron microscope (TEM) images of the EDC are shown in Fig. 4c and d. Phases can be separated by energy-disperse X-ray spectroscopy (EDX) analysis, as can be seen in Fig. 4e. Each phase exists as constrained structure in nano-scale. Co-conjugated Ni and YSZ are clearly observed at the edge of the composite particles (Fig. 4d). The relatively transparent phases are sintered Ni while the dark phases are conjugated YSZ phases.

Fig. 6 shows the electrical conductivity variations of the Ni–YSZ electrode depending on the number of thermal cyclings. The experimental conditions have been reported in a previous work by the authors [10]. The electrical conductivity represents the percolation of Ni phases. Uniform distribution of Ni phase is preferable for high electrical conductivity. The electrical conductivity of the anode made of NiO–YSZ mixing powder decreases continuously with further thermal cycling. After 50 thermal cyclings, the electrical conductivity decreased

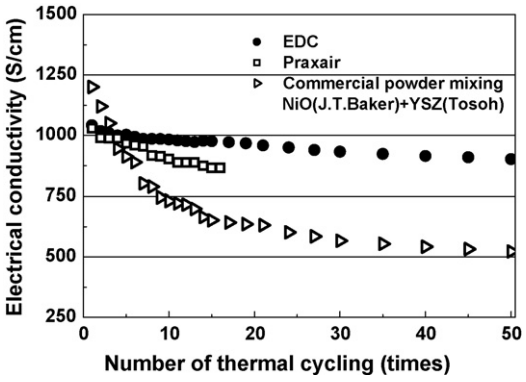

Fig. 6. Electrical conductivity variations of anodes depending on thermal cycling.

from 1208.8 to 522.7 S cm^{-1} (56.8% decrease). The conductivity of the commercial electrode material (Praxair) also exhibits rapid degradation with thermal cycling. However, the electrical conductivity of the EDC shows little change during 50 thermal cycling tests (11.4% decrease).

The contact between the ceramic and nickel tended to separate due to the different thermal expansion coefficients and low wettability [19]. This indicates that poor adhesion in the Ni/YSZ interface brings about separation of the surfaces instead of common interfaces (Ni/YSZ), which would be favorable for electrode reactions. However, as can be seen in Fig. 4b and c, TPBs are clearly observed in the EDC, and advantageously, the interface is continuous at every contact site between Ni and YSZ. This constrained and interpenetrated microstructure could be obtained by hetero-sintering of conjugated NiO and YSZ, which inhibits aging of the electrode microstructure at high temperature. The TPBs and interfaces are important factors with respect to performance and durability, as described later in this paper.

3.3. Performance and durability of a single cell

Shown in Fig. 7a is the total cell resistance of a single cell determined from impedance spectra as a function of operating time under open-circuit conditions. The polarization resistance of the initial state is 0.8 cm^2 at 800 °C. During 102 h of operation, no appreciable changes in resistance related to the aging of the electrode microstructure were detected. This unyielding cermet structure has its origin in the constrained and interpenetrated microstructure. Based on the tendency of the impedance data, the EDC is likely to maintain its durability.

Shown in Fig. 7b is the cell voltage and power density as a function of current density for a single cell composed of LSM-YSZ/YSZ/EDC. The maximum power density is 0.2, 0.6, and 1.2 W cm^{-2} at 600, 700, and 800 °C, respectively, in reactive gases of humidified hydrogen (200 cm^3 min^{-1}) with 3% H_2O and air (300 cm^3 min^{-1}). This constitutes noteworthy performance for SOFCs rooted in expanded TPBs, with high electrical conductivity (>1000 S cm^{-1}) and sufficient porosity (>40%) of EDCs.

Fig. 8 shows the results of a durability test performed under a static load of 1.0 A cm^{-2} at 800 °C. During 550 h of testing,

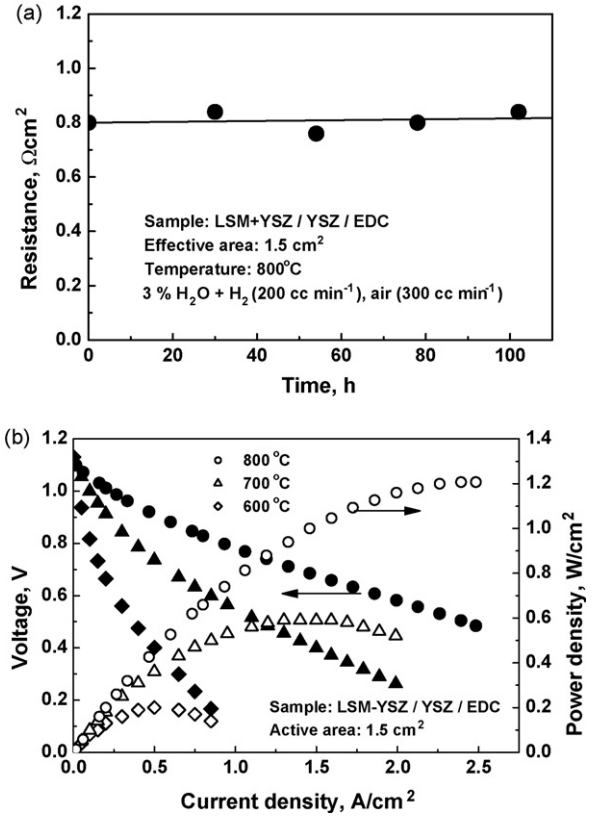

Fig. 7. (a) Total resistance of a single cell determined from impedance spectra as a function of operating time under open-circuit conditions and (b) cell voltage and power density as a function of current density for a single cell in reactive gases of humidified hydrogen (200 cm^3 min^{-1}) with 3% H_2O and air (300 cm^3 min^{-1}).

the corresponding cell voltage ranged from 0.799 to 0.802 and showed no degradation with an error of less than 0.2%. This enhanced durability is attributed to the microstructure stability, including TPBs, pores, and mutual arrangement of phases. During operation, densification and grain growth is inhibited because mobility in the heterogeneous region is sufficiently low,

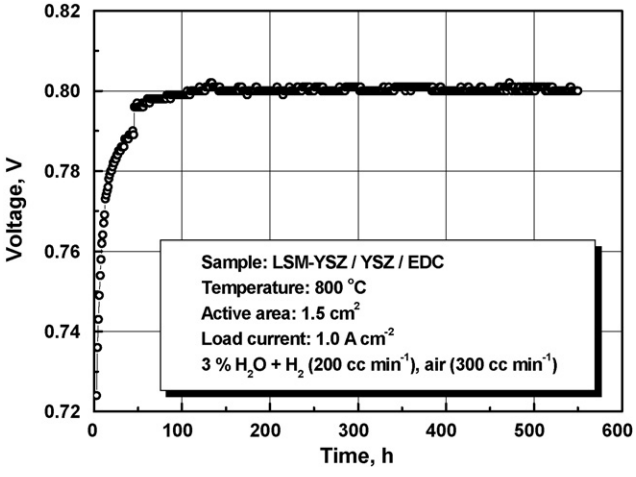

Fig. 8. Long-term stability of a single cell under a static load of 1.0 A cm^{-2} in reactive gases of humidified hydrogen (200 cm^3 min^{-1}) with 3% H_2O and air (300 cm^3 min^{-1}) at 800 °C.

which results in pore stability. These results demonstrate the superiority of the dual composite powder with respect to the realization of long-life SOFCs.

4. Conclusions

Degradation of the electrode microstructure at high temperatures was inhibited effectively with the proposed dual composite powder (nano-sized NiO and YSZ co-conjugated on YSZ particles). The durability stems from the uniform and solid interpenetrated cermet structure, particularly from the interface between the Ni and YSZ, which has been modified via nano-conjugation. A SOFC single cell made from the EDC exhibits high power densities of 0.2, 0.6, and 1.2 $W\,cm^{-2}$ at 600, 700, and 800 °C, respectively. The single cell shows excellent durability (zero degradation) under load of 1.0 $A\,cm^{-2}$ at 800 °C over 550 h of operation. The demonstrated performance and durability are promising and indicate feasible increased system reliability and system conciseness. The availability of such high performance and long life SOFCs may advance the date when they are put into practical use in applications such as residential and auxiliary power units.

Acknowledgement

This work was supported by the Core Technology Development Program for Fuel Cell of Ministry of Science and Technology and Korea Institute of Science and Technology Evaluation and Planning.

References

[1] S. Primdahl, M. Mogensen, J. Appl. Electrochem. 30 (2000) 247.
[2] D. Waldbillig, A. Wood, D.G. Ivey, J. Power Sources 145 (2005) 206.
[3] Y.C. Hsiao, J.R. Selman, Solid State Ionics 98 (1997) 33.
[4] D. Simwonis, F. Tietz, D. Stover, Solid State Ionics 132 (2000) 241.
[5] D. Waldbillig, A. Wood, D.G. Ivey, Solid State Ionics 176 (2005) 847.
[6] M. Mogensen, S. Skaarup, Solid State Ionics 86 (1996) 1151.
[7] M. Mogensen, S. Primdahl, M.J. Jorgensen, C. Bagger, J. Electroceram. 5 (2000) 141.
[8] P. Costamagna, P. Costa, V. Antonucci, Electrochem. Acta 43 (1998) 375.
[9] F.P.F. van Berkel, F.H. van Heuveln, J.P.P. Huijsmans, Solid State Ionics 72 (1994) 240.
[10] S.D. Kim, H. Moon, S.H. Hyun, J. Moon, J. Kim, H.W. Lee, Solid State Ionics 177 (2006) 931.
[11] Y. Sunagawa, K. Yamamoto, A. Muramatsu, J. Phys. Chem. B 110 (2006) 6224.
[12] P. Duran, J. Tartaj, F. Capel, C. Moure, J. Eur. Ceram. Soc. 23 (2003) 2125.
[13] S.K. Pratihar, A.D. Sharma, R.N. Basu, H.S. Maiti, J. Power Sources 129 (2004) 138.
[14] F.H. Wang, R.S. Guo, Q.T. Wei, Y. Zhou, H.L. Li, S.L. Li, Mater. Lett. 58 (2004) 3079.
[15] G. Gen, Z.X. Guo, C.K.L. Davies, Scr. Mater. 43 (2000) 307.
[16] J.W. Moon, H.L. Lee, J.D. Kim, G.D. Kim, D.A. Lee, H.W. Lee, Mater. Lett. 38 (1999) 214.
[17] T. Fukui, K. Murata, S. Ohara, H. Abe, M. Naito, K. Nogi, J. Power Sources 125 (2004) 17.
[18] D. Simwonis, H. Thulen, F.J. Dias, A. Naoumidis, D. Stover, J. Mater. Process. Technol. 92-93 (1999) 107.
[19] A. Tsoga, A. Naoumidis, P. Nikolopoulos, Acta Mater. 44 (1996) 3679.
[20] S.P. Jiang, J. Mater. Sci. 38 (2003) 3775.
[21] S.D. Kim, S.H. Hyun, J. Moon, J.H. Kim, R.H. Song, J. Power Sources 139 (2005) 67.
[22] X. Deng, A. Petric, J. Power Sources 140 (2005) 297.
[23] R.M.C. Clemmer, S.F. Corbin, Solid State Ionics 166 (2004) 251.
[24] V.V. Srdic, M. Winterer, H. Hahn, J. Am. Ceram. Soc. 83 (2000) 1853.
[25] V.S. Bakunov, A.V. Belyakov, Inorg. Mater. 32 (1996) 519.